

# Research Article

## DTI-based visualization strategies for the pyramidal tract

Frank Enders<sup>1\*,2</sup>, Dorit Merhof<sup>1,2</sup>, Peter Hastreiter<sup>1,2</sup>, Marc Stamminger<sup>2</sup>, Rudolf Fahlbusch<sup>1,3</sup>, Christopher Nimsky<sup>1,3</sup>

<sup>1</sup>Neurocenter, Department of Neurosurgery, University Hospital Erlangen, Germany

<sup>2</sup>Computer Graphics Group, University of Erlangen-Nuremberg, Germany

<sup>3</sup>Department of Neurosurgery, University Hospital Erlangen, Germany

GMS CURAC 2006;1:Doc07

provisional PDF

---

### Abstract

With the introduction of diffusion tensor imaging a method became available which is capable to detect major white matter tracts in-vivo. For the visualization of the data several techniques have been developed which, however, show various drawbacks for a comprehensive medical and technical analysis. Although fractional anisotropy maps and streamlines, typically denoted as fiber tracking, are widely used they are suboptimal in several situations of pre- and intraoperative application. Going beyond these standard approaches, several new and more advanced visualization techniques, namely directional volume growing, hulls and hardware-accelerated glyphs are introduced for an improved exploration of the pyramidal tract. The approaches have been evaluated with respect to diagnosis and therapy planning in neurosurgery. Overall, it is shown that the presented strategies for the visualization of diffusion tensor imaging data are capable to significantly support neurosurgical planning and intervention.

**Keywords:** diffusion tensor imaging, glyphs, fiber tracking, visualization, pyramidal tract

### Introduction

Based on diffusion tensor imaging (DTI) it became possible to obtain information about neuronal pathways in the human brain in-vivo. This is possible due to the strongly aligned microstructure, like cell membranes and the myelin sheath surrounding myelinated white matter, causing impediment of the water motion. To measure this restricted water diffusion, at least six datasets must be acquired, each with a gradient applied which is non-collinear with all other gradient directions (e.g.  $(\pm 1, 1, 0)$ ,  $(\pm 1, 0, 1)$ ,  $(0, 1, \pm 1)$ ). In combination with an additional reference dataset without any gradient information an equation system has to be solved to provide the 6 matrix entries of a symmetric  $3 \times 3$  diffusion tensor at each voxel. The respective eigensystem of this tensor describes the averaged diffusion distribution of water at an associated volume element. In case of strong diffusion, as it occurs in areas of nerve tracts, the principal eigenvector gives the orientation of nerve fibers [1], [2], [3].

Avoiding postoperative neurological deficits by preserving eloquent brain areas is a major demand in neurosurgery. Functional brain areas can be successfully localized by identifying them with methods such as magnetoencephalography (MEG) and functional magnetic resonance imaging (fMRI). However, while these modalities only show function on the cortex, DTI shows white matter tracks lying deeper in the brain which connect functional structures on the cortex [4], [5], [6], [7]. Since they represent important functional structures themselves, they have to be preserved during surgery to avoid postoperative neurological deficits.

---

\*Corresponding author: Frank Enders, Neurozentrum, Neurochirurgie, Schwabachanlage 6, 91054 Erlangen, Tel.: +49-9131-8534265, Fax: +49-9131-8534271, eMail: enders@informatik.uni-erlangen.de

In this work, we present a collection of new and more advanced visualization techniques focusing on the improved exploration of the pyramidal tract based on DTI data. The basic methods, i.e. Fractional Anisotropy Maps, Glyphs, and Fiber Tracking, were reimplemented for reasons of comparison while Directional Volume Growing and Pathway Hulls have been originally developed and implemented by our group and Evenly Spaced Streamlines were ported for the use with DTI data. All approaches were evaluated with respect to diagnosis and therapy planning in neurosurgery and contribute to a more comprehensive understanding and analysis of the individual pathology of a patient.

## Methods

### Imaging

Single-shot spin-echo diffusion weighted echo planar imaging on a 1.5 T MR scanner (Magnetom Sonata, Siemens Medical Solutions, Erlangen, Germany) was used for DTI. The sequence parameters were: TE 86 ms, TR 9200 ms, matrix size 128 x 128, FOV 240 mm, slice thickness 1.9 mm, bandwidth 1502 Hz/Px. A diffusion weighting of 1000 s/mm<sup>2</sup> (high b value) was used. One null image (low b value: 0 s/mm<sup>2</sup>) and six diffusion weighted images were obtained with the diffusion-encoding gradients directed along the following axes ( $\pm 1, 1, 0$ ), ( $\pm 1, 0, 1$ ), and ( $0, 1, \pm 1$ ). The voxel size was 1.9 x 1.9 x 1.9 mm<sup>3</sup>; 60 slices with no intersection gap were measured. Applying 5 averages the total DTI measurement required 5 minutes and 31 seconds.

### Visualization strategies

#### Fractional anisotropy maps

For the analysis of the DTI data, slice-based fractional anisotropy (FA) maps are commonly in use [8], [9]. Conceptually, the resulting FA maps are similar to other tomographic images. However, the value mapping is different. While magnetic resonance imaging (MRI) depicting anatomy shows different types of hydrogen relaxation, FA represents the reconstructed anisotropy of the tissue. Areas featuring a highly anisotropic behavior are bright and those with mainly isotropic diffusion, i.e. unrestricted water diffusion, are dark. In addition to that, the direction of the principal eigenvector of the corresponding tensor can be mapped to color. This allows expressing the direction of the diffusion together with the intensity. Figure 1a shows a color mapping where the anterior-posterior, left-right and head-feet direction of the diffusion are mapped into RGB color space respectively. As a limitation, FA maps are restricted to 2D slice representations and reduce the data from tensor to a vector and finally even to a scalar metric.

#### Glyphs

In order to overcome the constraints of FA maps, glyphs were used for improvement [10]. In contrast to slice-based FA maps, where a voxel can only show color values, glyphs express the data information more entirely by their geometrical shape. They show orientation and intensity of diffusion directly by their orientation and size. Independent of its actual shape a glyph is oriented according to the perpendicular eigenvectors of the tensor while the size of its axes is related to the corresponding eigenvalues (Figure 1b).

#### Directional volume growing

In addition to glyphs, directional volume growing is another technique which directly takes the underlying voxel structure into account. It allows extracting structures satisfying certain expansion criteria which enable the estimation of the overall white matter occurrence [11].

Typical volume growing algorithms start from a seed point and spread out within the volume until some terminating criterion is reached. For directional volume growing the spread strategy has been modified. While standard volume growing equally expands in all directions equally, directional volume growing also considers the local tensor shape and the FA value serves as termination criterion. Concretely, the algorithm marks all voxels in the vicinity of the original voxel which fit the diffusion distribution at that voxel and fulfill the FA criterion. The starting region is defined as a region of interest

(ROI) similar to fiber tracking. The resulting structure is a set of connected voxels incorporating all areas of the data which satisfy the given criteria (Figure 1c).

### **Fiber tracking**

In order to further emphasize the connectivity of voxels in relation to white matter tracts, streamlines based on fiber tracking are commonly used for DTI visualization. The concept is based on the tracing of particles in a vector field known from computational fluid dynamics [12]. The resulting path of each particle forms a line which is closely linked to the underlying tissue and therefore represents a model for the related major white matter tracts [13], [14], [15], [16], [17], (Figure 1d).

To fit in the concept of vector field tracing, each tensor of the volume is reduced to its principal eigenvector. The tracking algorithm itself starts from a preliminarily defined seed point. Thereafter, tracking is performed in direction of the starting eigenvector as well as in the opposite direction. Thereby, a single step consists of the trilinear interpolation of the tensor at the current position, the eigensystem decomposition and the final integration of the step which is performed by 4th order Runge-Kutta [18]. The step size was set to a fixed value which is a quarter of the voxel diagonal. As an additional issue, the eigenvector may point in either direction of the diffusion. However, since the direction is of no importance for the tracking, the eigenvectors are inverted, if they are oriented opposite to the current streamline direction. Propagation stops if the associated FA value which represents the degree of anisotropic diffusion falls below a certain threshold. To generate a tracking of the whole brain seed points are selected throughout the entire dataset according to a certain user defined FA value, as well.

### **Evenly spaced streamlines**

Reconsidering the results of fiber tracking it occurs that the streamlines are often unequally distributed which leads to a misleading impression of the neuronal pathways. This is due to the fact that each seed point results in one streamline. This means, the representation of the underlying vector field is only sparse. This means that divergent areas in the flow field, e.g. forks, are very likely to occur as blind spots in case that no seed points are placed in this area. To prevent such an insufficient representation ESS was introduced. The basic principle of ESS is to calculate streamlines until a user-defined density level is reached [19]. Thereby, a regular distribution of the streamlines is achieved and areas with a sparse distribution of streamlines are filled. The ESS-algorithm computes an initial streamline and chooses new seed points in its vicinity with a distance  $d_{seed}$ . Starting at these seed points, the new streamlines are propagated in both forward and backward direction until they come closer than  $d_{sep}$  to each other or until the boundary of the volume is reached. To avoid the new streamline to terminate instantly in the first step,  $d_{seed}$  is set slightly higher than  $d_{sep}$ .

To improve evenly spaced streamline tracking of the whole brain, we adapted the approach to ROI-based tracking. Thereby, in a first pass standard ROI fiber tracking using evenly spaced streamlines is performed. In a second pass, sparsely filled regions are recomputed with the approach of evenly spaced streamlines based on the results of the first pass. With this technique, the concept of evenly spaced streamlines was adapted to ROI tracking providing dense tracts capturing the features within the data more precisely (Figure 1e).

### **Pathway hulls**

Line rendering has one significant drawback in this context. To get the extension of a nerve tract one must estimate the border of the fiber bundle. To overcome this, a clear and unambiguous surface representation is suggested providing a hull which describes the boundary of the nerve tract based on the results of streamline calculations [20]. In this context, streamlines serve as basis structures which are then wrapped by a surface, regardless of the generating algorithm. Using ROIs or automatic clustering, a certain white matter structure is selected and the corresponding streamlines are bundled. Subsequently, a centerline is determined describing the course of the entire bundle. The bounding curves, which form the skeleton of the hull, are generated by calculating the points of intersection of the streamlines contained in the bundle with planes perpendicular to the centerline. Each single curve lies in one of these planes. Due to the 2D nature of the curve, their definition based on the set of points can be achieved by the Graham Scan algorithm [21]. In a final step, the curves are connected to a mesh, representing the boundary surface. To achieve an expressive surface representation, it is also essential to apply Phong lighting [22] since it significantly enhances the impression of depth and

thereby assists the proper examination of the surface by emphasizing detailed surface structures (Figure 1f).

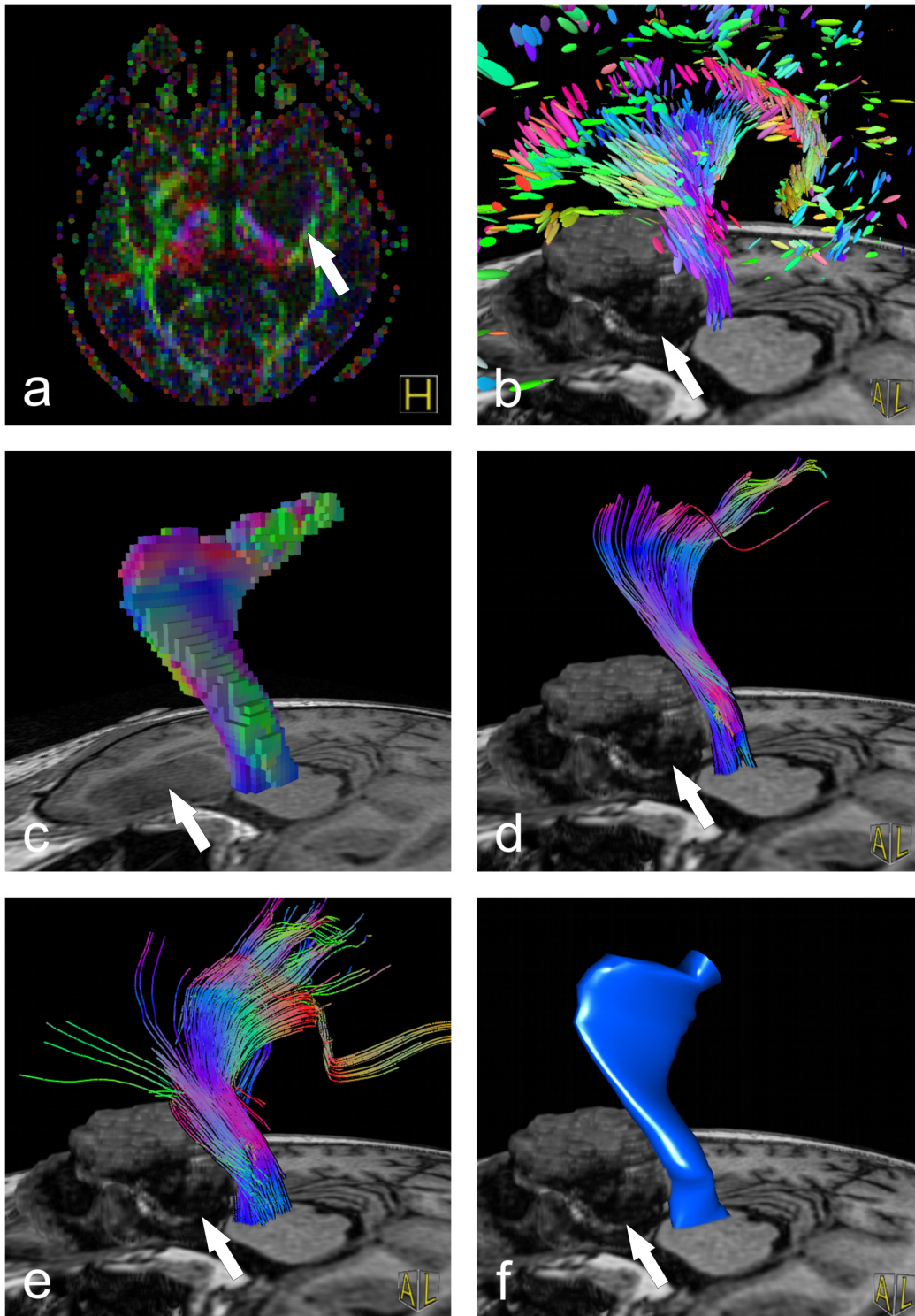


**Figure 1: Visualization of the right pyramidal tract with the presented visualization approaches on a 66 year old male patient with a lesion (arrows) on the right side close to the brainstem. (a) FA map, (b) Glyphs, (c) Directional Volume Growing, (d) Fiber Tracking, (e) Evenly Spaced Streamlines, (f) Hull. The images b and d-f combine the visualization of the pyramidal tract with the direct volume rendering of a T1-weighted MR scan where the tumor is manually segmented. The coloring of all images except f is following the standard way of coloring DTI. The direction of the major eigenvector is directly mapped into RGB color space which leads to a red coloring in case of a major eigenvector collinear to the x-axis of the dataset and green and blue coloring for the y- and z-axis respectively. Moreover, standard Gouraud Shading and lighting is applied.**

## Results

### Datasets

Each of the addressed visualization strategies was applied to 12 datasets of patients undergoing glioma surgery. For all computation and visualization tasks a standard PC (Intel 3.0 GHz) with 2 GB main memory and a NVIDIA GeForce 6800 Ultra graphics card, providing 256 MB graphics memory, was used. All presented approaches were implemented into an in-house visualization application developed for analysis purpose of medical data at the Neurocenter, Erlangen.

Since interactivity is guaranteed for all approaches on this machine, user interaction was not restricted and therefore did not influence the comparison. In addition to the general applicability of the presented approaches for DTI data, the focus of this evaluation was a classification of the different DTI visualization techniques with respect to the provided representation of the pyramidal tract.

Figure 1 shows an overview of all presented methods on a 66 year old male patient with a glioma. The lesion is situated on the right side very close to the brainstem and therefore in direct contact to the right pyramidal tract. In addition to the different visualization techniques, the images b and d-f contain a volume rendering of an anatomical MRI dataset with a manually segmented tumor. Image c possesses a corresponding slice rendering of the anatomical data for the purpose of navigation. Figure 1a shows a FA map of the DTI data. The axial slice is positioned in a way that it cuts the tumor. The tumor, marked by the arrow, appears darker due to isotropic diffusion in this kind of tissue. The bright violet-blue area on the lower left of the dark spot indicates the pyramidal tract. Coloring follows the principal eigenvector which was adapted for the images b-e as well. The representation of the white matter tracts in Figure 1b was generated by the use of glyphs. To avoid overloading of ellipsoids, the DTI data was restricted to a stack of 12 sagittal slices for rendering enclosing the pyramidal tract which is depicted by the blue ellipsoids emerging out of the brainstem. The glyphs forming a red arc are a part of the corpus callosum. Figure 1c presents the results of directional volume growing for a seed region at the relevant nerve tract. The blocky appearance of the structure indicates the underlying voxel resolution. The streamlines displayed in Figure 1d are a standard approach for the visualization of the pyramidal tract. This technique is extremely useful to show the close relation of tumor and neuronal pathway. Figure 1e shows ESS as an extension of standard fiber tracking. The resulting streamlines are evenly distributed and the impression of denser and sparser areas is avoided. Finally, Figure 1f depicts the pathway hull of the pyramidal tract which allows observing a clear border and 3D object.

A couple of different setups for glyph rendering are presented in Figure 2. The unrestricted display of all ellipsoids leads to useless images (a). For improvement, the user can raise the threshold for FA to eliminate ellipsoids representing isotropic diffusion (b). An interesting alternative is the reduction towards a single slice of the DTI dataset, e.g. an axial or a sagittal slice (c and d respectively).

Figure 3 shows a comparison of different density levels produced by the ESS algorithm. On the left, the result of a standard fiber tracking is given as a reference. In the middle, a dense representation of the whole brain is generated while the right line-set is extremely sparse, displaying only the coarse structures.

Figure 4 presents the comprehensive display of a hull, achieved by wrapping a surface around a fiber bundle (right). The basic streamline bundle is shown on the left, while the image in the middle displays a semi-transparent rendering of the hull which allows viewing the inside of the streamlines. This is especially useful for the evaluation of the hull and the potential overestimation of the bundle by the boundary curves.

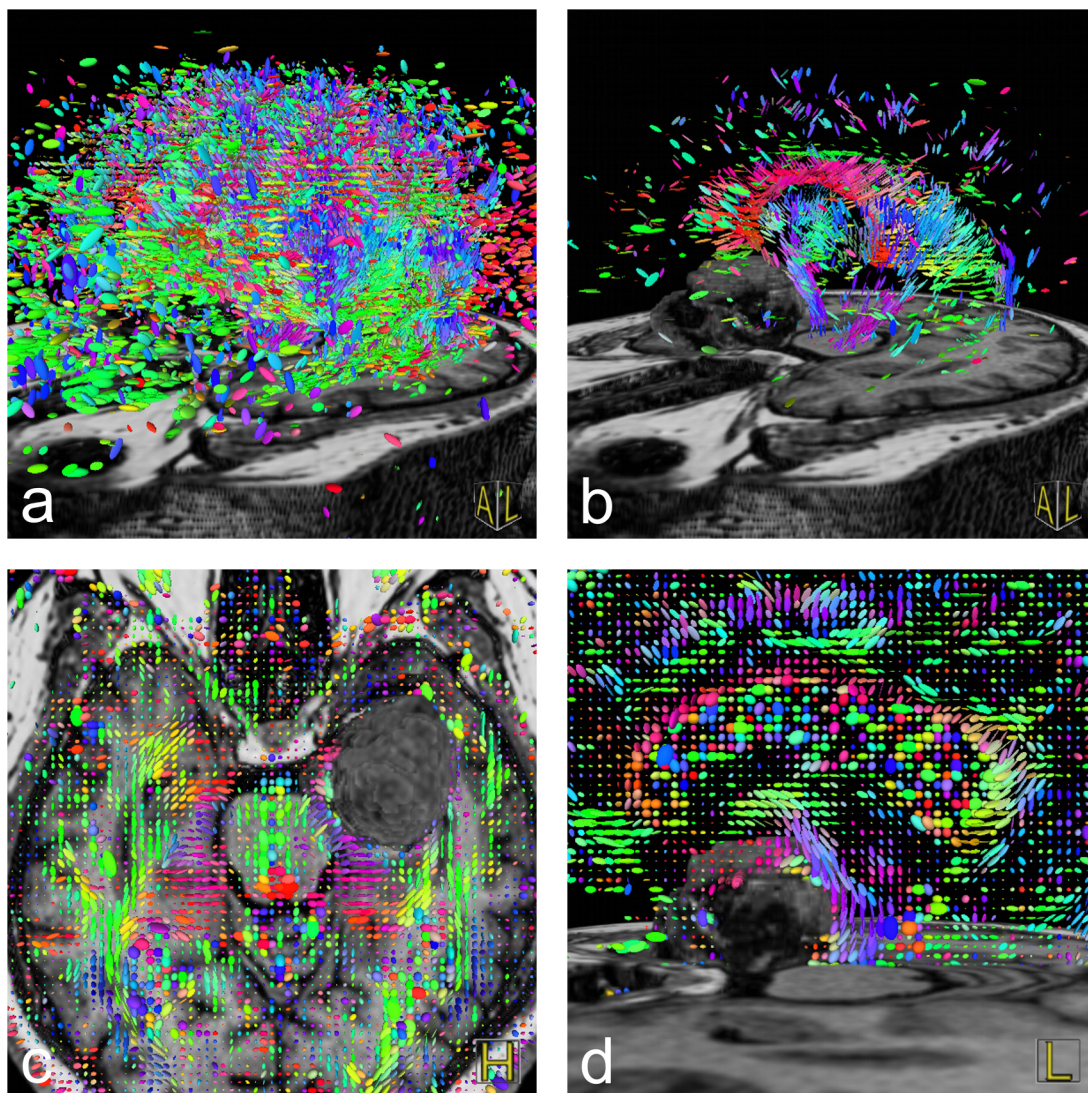


Figure 2: Glyph-based visualization of the patient with different parameter settings: (a) 3D rendering of all ellipsoids with a corresponding FA value greater than 0.5, (b) same rendering with FA greater than 0.75, (c) all ellipsoids of a single axial slice, (d) likewise image of a sagittal slice.

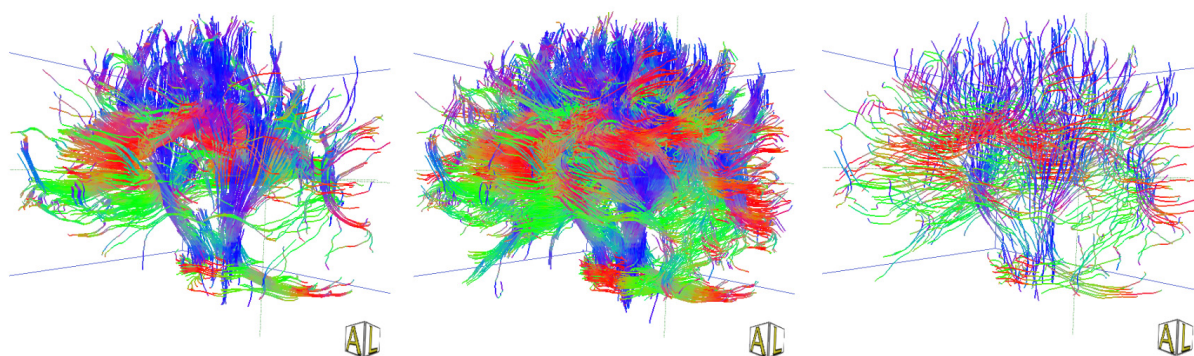
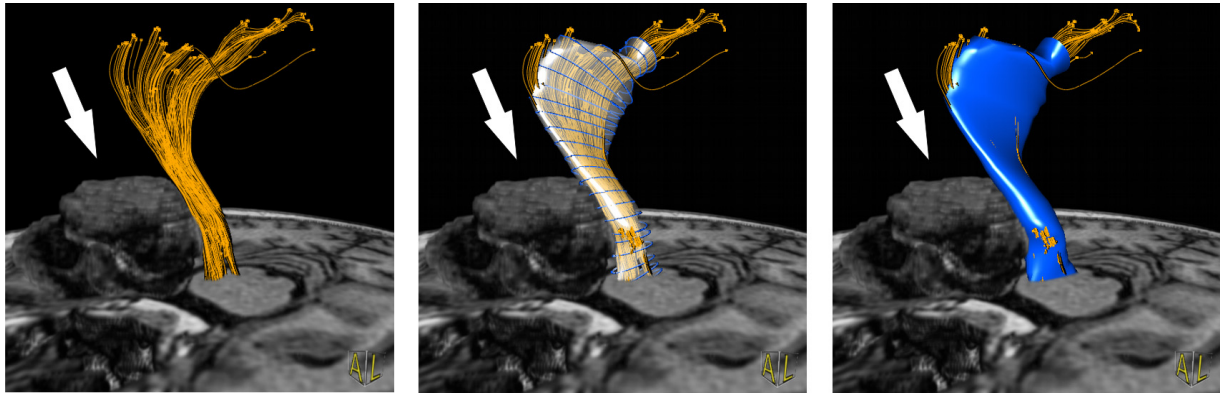


Figure 3: Different streamline representations: standard fiber tracking result (left), dense streamlines generated with the ESS algorithm with low  $d_{seed}$  and  $d_{sep}$  values (middle), high parameter values for ESS (right).



**Figure 4: Pathway hull visualization of DTI data. After streamline calculation (left) the entire bundle is wrapped with a hull which is rendered either in semi-transparent (middle) or opaque mode (right). Additionally, an axially clipped volume rendering is integrated which allows better navigation especially with respect to the manually segmented tumor (arrow). In this case, coloring of the lines is restricted to single-color due to better perception in combination with the hull.**

## Comparison

Based on the different visualization strategies and the experience from neurosurgery, Table 1 summarizes the clinical suitability of the different visualization techniques. FA maps and glyph representations are voxel based strategies and are most adequate for a local investigation of specific areas. With some restrictions, also directional volume growing can be used for this kind of examination but it also gives global information. The analysis of major white matter tracts heavily relies on the spatial context which is especially supported by all methods based on fiber tracking. Since the planning of neurosurgery is also based on questions concerning spatial relations, fiber tracking approaches are predestined for pre- and intraoperative application. Some special problems occur for the appliance in the OR. Mainly, the overlay in the microscope restricts the type of visualization to a simple schematic representation. Therefore, directional volume growing and hulls are most suitable since they allow extracting bounding silhouettes of the structures suitable for overlay purpose.

**Table 1: Different visualization approaches and their benefit for the examination of the pyramidal tract. (+) stands for a generally good suitability of the approach for the respective task while (-) indicates inappropriateness. In case of (o) the approach may be suitable but not in general.**

	Technical analysis		Medical application	
	detailed analysis	spatial analysis	preoperative planning	intraoperative visualization
FA	+	-	O	-
Glyphs	+	O	-	-
Directional volume growing	O	+	+	+
Fiber tracking	-	+	+	-
Evenly spaced streamlines	-	+	+	-
Pathway hulls	-	+	+	+

## Preprocessing

The time required for preprocessing is an important issue for DTI data analysis. All visualization techniques have in common the calculation of the 2<sup>nd</sup> order tensor based on the diffusion weighted images. On our PC the calculation took almost 10 seconds. Considering the small resolution of 128 x 128 x 60 of the DTI datasets this is relevant since the algorithm behaves linear in time and memory consumption. Subsequently, an eigensystem evaluation is required for all visualization strategies. While FA mapping only needs the eigenvalues all other techniques rely on the evaluation of at least the principal eigenvector. In addition to that, glyphs need the 2<sup>nd</sup> eigenvector to determine the orientation of the glyph. Regarding time, the evaluation of the eigensystem is comparable to the tensor calculation which means that the actual preprocessing time for a glyph representation rises up to 20 seconds. Afterwards, directional volume growing, based on the same eigensystem evaluation, can be performed almost in real time. The timing for fiber tracking heavily depends on the chosen parameters. For a FA value of 0.5, the resulting time for a whole brain tracking is about 10 seconds and results to approximately 7000 streamlines. Finally, hull generation for a single fiber bundle can be achieved on an average of 0.2 seconds. Overall, the complete process takes about 40 seconds without user interaction. This is acceptable even for intraoperative use. However, it must be considered that increasing data resolution will have a strong impact on the given numbers making performance optimization a critical issue.

## Discussion

### FA maps

The most obvious advantage of FA maps is their similarity to common anatomical slice images since physicians are familiar with this kind of 2D representation. Besides, especially the comparatively high degree of accuracy is of certain value for the evaluation of DTI data. Therefore, FA maps are of major interest for detailed analysis of certain structures and abnormalities [9], [23]. On the other hand, the lack of connectivity between each slice prevents an efficient spatial analysis of neuronal pathways, especially in case of the pyramidal tract. This makes the technique insufficient for a macroscopic analysis of nerve connectivity and tract alignment.

### Glyphs

Although there are different choices for the shape of a glyph, ellipsoids are most frequently used since the visual impression is far more intuitive than other geometrical objects such as octahedrons. However, ellipsoids are by far computationally more expensive than simpler shapes like cuboids since the triangulation of the geometry results in a fine mesh which leads to higher rendering costs. This was overcome with new algorithmic approaches exploiting functionality of most recent PC graphics hardware allowing even high numbers of tensor ellipsoid in real time [24]. An even more appropriate shape for tensors are superquadric tensor glyphs which provide a better and less ambiguous spatial impression [25]. However, superquadrics are computationally even more expensive and are currently not implemented on graphics hardware.

The advantage of glyph-based techniques is the fact that the entire tensor information is visualized. Therefore, they are especially appropriate for a detailed examination of the data. However, similar to FA maps, the results of this visualization approach are difficult to interpret in terms of underlying nerve structures since no global connectivity information is provided. Consequently, a combination with other visualization techniques such as fiber tracking is recommended to obtain a meaningful representation. In addition to that, clipping (Figure 2b) or slice views (Figure 2c and d) of glyphs are necessary to avoid an overloading and cluttering of information in 3D representations. For the special appliance on pyramidal tracts, the glyphs are of minor importance since the macroscopic analysis of nerve tracts is not adequately supported similar to FA maps.

### Directional volume growing

The advantage of directional volume growing approaches over general isosurface based approaches is the fact that a connected volume is generated. The fragmented nature of an isosurface based on a FA volume makes it difficult to clearly identify connectivity information which is important for surgery. In

contrast to that, volume growing produces a connected volume without any detached parts which also allows performing volumetry. In order to further enhance the visual impression, an isosurface can be calculated based on the results of directional volume growing. Thereby, an improved representation of the surface can be obtained [11]. In summary, directional volume growing reveals the internal structure of the nerve tract in a plausible manner.

## Fiber tracking

The primary objective of fibers is the comprehensive 3D visualization of the nerve tract which reveals the location of fibers relative to a tumor and anatomy [13], [14]. As a drawback, lines are limited in a way that they can only illustrate a direction. Additional information may be encoded with color or, in case of hyper-streamlines, in shape but still geometrical features of an underlying structure can only be estimated.

For the integration of the particle trace, different integration schemes can be applied. In case of Euler integration, the propagation of the streamlines follows the principal eigenvector of the tensor. However, due to numerical accuracy issues, higher order integration schemes like Runge-Kutta are superior to the Euler approach [18]. As a drawback, these schemes are computationally more expensive since they need repeated tensor interpolation and evaluation. In any case, since the field of the principal eigenvectors does not correspond to a flow field, we found it more convenient to choose a sufficiently low fixed step size instead of an adaptive adjustment which prevents the missing of sharp bends

Overall, streamlines are the current state of the art method to visualize DTI data [16], [17]. The common ground of lines and nerves thereby supports the intuitive understanding. Though, one must distinguish between tracked fibers, which are the result of a flow experiment, and the actual nerve fibers, which cannot be explicitly extracted due to the low resolution of the data. Being aware of the differences between real axons and the rendered lines, representing a simulation result on coarse data, they are a powerful tool for the exploration of internal brain structures in-vivo. Especially in the case of the pyramidal tract and a tumor situated nearby, fiber tracking is a valuable supplement to other diagnose and planning methods. Overall, the ability to distinguish between different major white matter tracts allows the surgeon performing a more precise intervention.

## Evenly spaced streamlines

ESS is an important improvement over the conventional fiber tracking approach. Due to the diverging nature of tract systems, the density of streamlines produced by standard fiber tracking varies over the domain without control resulting in sparse areas as well as cramped regions. Thereby, it is important to mention that dense areas in the fiber tracing result are not necessarily more important. In fact it is only a sign for a more distinct main direction of the neural pathways in the area. Areas with diverging directions, e.g. areas of crossing pathways, would lead to a more sparse representation. However, thus areas are considered equally important by clinicians. To overcome this problem, ESS rearranges the streamlines by terminating fibers falling below a certain distance to each other and starting new ones with appropriate spacing ensuring better visual perception of the nerve tract [19], [26]. Since whole brain fiber tracking can be performed in just a few seconds, the effort for the calculation of 2 or 3 more passes of fiber tracking is justified. As can be seen in Figure 3, the quality and interpretability increases considerably when using the ESS approach. Overall, ESS provides a more complete illustration of the actual distribution of the neural pathways.

## Hulls

The introduction of ESS improves the visualization in a way that the effect of cluttered lines is reduced. Nevertheless, it is hard to estimate the border of a certain nerve tract which is important for neuronavigation. This can be efficiently overcome by calculating a hull which wraps a complete fiber bundle [20]. Thereby, the representation of the nerve tract is accomplished in a more suitable manner since lines are not capable to provide an easy to interpret border. Instead, they require an interpretation of the rendered images in a way that the user has to estimate the volume and the border of the tract of interest. Therefore, the hulls are superior to streamlines since they determine a precise possible border between function and surrounding tissue. Accordingly, this approach is very suitable for the examination of the pyramidal tract during diagnosis and planning. In addition to that, a direct visualization of such representations within the surgical field can be easily achieved by visualizing

them on semi-transparent mirrors provided in operating microscopes. Thereby, the silhouette of the hull can easily be extracted in the focal plane of the microscope. The automatic clustering of a whole brain tracking, optionally used for the hulls, is currently not an option due to missing medical meaning and an average computation time of 90 minutes per case.

## Conclusions

The change in visualization strategies from detailed voxel-based approaches to more comprehensive methods is highly relevant for neurosurgery since these new techniques allow an easier identification of underlying nerve structures.

Especially for the planning of neurosurgery, more abstract representations of the neuronal pathways are valuable. The ability to incorporate the visualization results into the intraoperative process is another useful possibility which may help to allow removal of tumors adjacent to eloquent brain areas with low morbidity.

Overall, the presented approaches provide valuable support for the planning of neurosurgical intervention and the intervention itself.

## Acknowledgements

This work was supported by the German Research Foundation in the context of SFB 603, Project C9 and the Graduate Research Center "3D Image Analysis and Synthesis". We would like to thank Stefanie Kreckel, RT, for her technical support in MR imaging.

---

## References

1. Basser P, Mattiello J, LeBihan D. MR diffusion tensor spectroscopy and imaging. *Biophys J*. 1994;66(1):259-67.
2. Cruz Junior L, Sorensen A. Diffusion tensor magnetic resonance imaging of brain tumors. *Neurosurg Clin N Am*. 2005;16(1):115-34.
3. Le Bihan D, van Zijl P. From the diffusion coefficient to the diffusion tensor. *NMR Biomed*. 2002;15(7-8):431-4.
4. Clark CA, Barrick TR, Murphy MM, Bell BA. White matter fiber tracking in patients with space-occupying lesions of the brain: a new technique for neurosurgical planning? *Neuroimage*. 2003;20(3):1601-8.
5. Holodny A, Schwartz T, Ollenschleger M, Liu W, Schulder M. Tumor involvement of the corticospinal tract: diffusion magnetic resonance. *J Neurosurg*. 2001;95(6):1082.
6. Nimsy C, Ganslandt O, Hastreiter P, Wang R, Benner T, Sorensen AG, et al. Preoperative and intraoperative diffusion tensor imaging-based fiber tracking in glioma surgery. *Neurosurgery*. 2005;56(1):130-7; discussion 138.
7. Nimsy C, Ganslandt O, Hastreiter P, Wang R, Benner T, Sorensen AG, et al. Intraoperative diffusion-tensor MR imaging: shifting of white matter tracts during neurosurgical procedures - initial experience. *Radiology*. 2005;234(1):218-25.
8. Le Bihan D, Mangin J, Poupon C, Clark C, Pappata S, Molko N, et al. Diffusion tensor imaging: concepts and applications. *J Magn Reson Imaging*. 2001;13(4):534-46.
9. Westin C-F, Maier SE, Mamata H, Nabavi A, Jolesz FA, Kikinis R. Processing and visualization for diffusion tensor MRI. *Med Image Anal*. 2002;6(2):93-108.
10. Pierpaoli C, Jezzard P, Basser PJ, Barnett A, Di Chiro G. Diffusion tensor MR imaging of the human brain. *Radiology*. 1996;201(3):637-48.
11. Merhof D, Hastreiter P, Nimsy C, Fahlbusch R, Greiner G. Directional Volume Growing for the Extraction of White Matter Tracts from Diffusion Tensor Data. In: Robert L. Galloway Jr. KRC, editor. *Medical Imaging 2005: Visualization, Image-Guided Procedures, and Display*. San Diego, CA, USA: SPIE; 2005. p. 165-72.
12. Darmofal D, Haimes R. Visualization of 3-D Vector Fields: Variations on a Stream. In: *Proceedings AIAA 30 th Aerospace Science Meeting and Exhibit*; 1992.

13. Basser PJ, Pajevic S, Pierpaoli C, Duda J, Aldroubi A. In vivo fiber tractography using DT-MRI data. *Magn Reson Med*. 2000;44:625-32.
14. Mori S, Zijl Pv. Fiber tracking: principles and strategies - a technical review. *NMR Biomed*. 2002;15:468-80.
15. Stieltjes B, Kaufmann W, van Zijl P, Fredericksen K, Pearlson G, Solaiyappan M, et al. Diffusion tensor imaging and axonal tracking in the human brainstem. *Neuroimage*. 2001;14(3):723-35.
16. Vilanova A, Berenschot G, Pul Cv. DTI Visualization with Streamsurfaces and Evenly-Spaced Volume Seeding. In: *Proc. Joint EG/IEEE TCVG VisSym*; 2004. p. 173-182.
17. Zhukov L, Barr A. Oriented Tensor Reconstruction: Tracing Neural Pathways from Diffusion Tensor MRI. In: *Proc. IEEE Visualization*; 2002.
18. Kutta W. Beitrag zur näherungsweise Integration totaler Differentialgleichungen. *Z Math Phys*. 1901;46:435-53.
19. Merhof D, Sonntag M, Enders F, Hastreiter P, Fahlbusch R, Nimsky C, et al. Visualization of Diffusion Tensor Data using Evenly Spaced Streamlines. In: *Vision, Modeling, and Visualization*; 2005. p. 79-86.
20. Enders F, Sauber N, Merhof D, Hastreiter P, Nimsky C, Stamminger M. Visualization of White Matter Tracts with Wrapped Streamlines. In: *Proceedings of IEEE Visualization 2005: IEEE*; 2005. p. 51-8.
21. Graham RL. An Efficient Algorithm for Determining the Convex Hull of a Finite Planar Set. *Inf Process Lett*. 1972;1(4):132-3.
22. Foley JD, Dam Av, Feiner SK, Hughes JF. *Computer graphics: principles and practice (2nd ed.)*: Addison-Wesley Longman Publishing Co., Inc.; 1990.
23. Bihan DL, Mangin J-F, Poupon C, Clark CA, Pappata S, Molko N, et al. Diffusion Tensor Imaging: Concepts and Applications. *J Magn Reson Imaging*. 2001;13:534-46.
24. Enders F, Iserhardt-Bauer S, Hastreiter P, Nimsky C, Ertl T. Hardware-Accelerated Glyph Based Visualization of Major White Matter Tracts for Analysis of Brain Tumors. In: Robert L. Galloway Jr. KRC, editor. *Medical Imaging 2005: Visualization, Image-Guided Procedures, and Display*. San Diego, CA, USA: SPIE; 2005. p. 504-11.
25. Ennis DB, Kindlman G, Rodriguez I, Helm PA, McVeigh ER. Visualization of tensor fields using superquadric glyphs. *Magn Reson Med*. 2005;53(1):169-76.
26. Jobard B, Lefer W. Creating Evenly-Spaced Streamlines of Arbitrary Density. In: *Proc. 8th Eurographics Workshop in Scientific Computing*. Boulogne sur Mer, France; 1997. p. 45-55.